Molecular Biology of the Cell
Vol. 21, 778–790, March 1, 2010

# Glycolipid Trafficking in *Drosophila* Undergoes Pathway Switching in Response to Aberrant Cholesterol Levels

**Ralf Hortsch,*†‡ Esther Lee,†‡ Nandanan Erathodiyil,‡ Sarita Hebbar,‡§ Steffen Steinert,‡‖ Jun Yu Lee,¶ Doreen See Kin Chua,¶# and Rachel Kraut¶**

‡Institute of Bioengineering and Nanotechnology, Agency for Science, Technology, and Research, Singapore 138669; and ¶School of Biological Sciences, Nanyang Technological University, Singapore 639798

Submitted January 8, 2009; Revised November 24, 2009; Accepted December 22, 2009
Monitoring Editor: Marcos Gonzalez-Gaitan

**In lipid storage diseases, the intracellular trafficking of sphingolipids is altered by conditions of aberrant cholesterol accumulation. *Drosophila* has been used recently to model lipid storage diseases, but the effects of sterol accumulation on sphingolipid trafficking are not known in the fly, and the trafficking of sphingolipids in general has not been studied in this model organism. Here, we examined the uptake and intracellular distribution of a fluorescent glycolipid analog, BODIPY-lactosyl-ceramide, in *Drosophila* neurons. The uptake mechanism and intracellular trafficking route of this simple glycolipid are largely conserved. Our principle finding is that cholesterol steers trafficking of the glycolipid between Golgi, lysosome, and recycling compartments. Our analyses support the idea that cholesterol storage in *Drosophila* triggers a switch in glycolipid trafficking from the biosynthetic to the degradative endolysosomal pathway, whereas cholesterol depletion eliminates recycling of the glycolipid. Unexpectedly, we observe a novel phenomenon we term "hijacking," whereby lactosyl-ceramide diverts the trafficking pathway of an endocytic cargo, dextran, completely away from its lysosomal target. This work establishes that glycolipid trafficking in *Drosophila* undergoes changes similar to those seen in mammalian cells under conditions of cholesterol storage and therefore validates *Drosophila* as a suitable model organism in which to study lipid storage diseases.**

## INTRODUCTION

*Drosophila* has recently been adopted for the modeling of neurodegenerative lipid storage diseases, including Niemann-Pick, neuronal ceroid lipofuscinoses, and Tay Sach's disease (Min and Benzer, 1997; Nakano *et al.*, 2001; Huang *et al.*, 2005; Myllykangas *et al.*, 2005; Phillips *et al.*, 2008). The utility of the fly as a model in studying these diseases and examining their effects on lipid-trafficking routes will depend strongly on the development of lipid tracers that accurately report on the affected trafficking pathways. As in mammalian cellular models (Marks and Pagano, 2002), fluorescent glycosphingolipid analogs are potentially valuable tools in the characterization of fly models for lipid storage disorders and other diseases that affect lipid storage and metabolism, such as Alzheimer's disease (Puglielli *et al.*, 2003; Cutler *et al.*, 2004; Wolozin, 2004; Maxfield and Tabas, 2005).

The aim of this study was to address two key issues, as a starting point for further studies using the *Drosophila* nervous system as a platform for studying lipid trafficking defects. First, we asked whether fluorescently tagged glycosphingolipids (GSLs), which have been used to study lipid trafficking in human cell types, are taken up and trafficked by *Drosophila* cultured neurons; and second, whether the trafficking of these GSLs is similarly affected by lipid perturbations (e.g., cholesterol storage) as their mammalian counterparts. Because these lipids are known to accumulate along with cholesterol in the endocytic compartments of Niemann-Pick diseased cells and in other lipid storage diseases, it is important to be able to follow their trafficking routes under normal and perturbed conditions such that one can better describe the cellular pathology and to evaluate the effectiveness of potential treatments.

To address the first question of how GSLs are trafficked in *Drosophila,* we use fluorescent dipyrromethene boron difluoride (BODIPY)-coupled analogs of a simple glycolipid, lactosyl-ceramide (lac-Cer), to show that a *Drosophila* neuronal cell line incorporates and traffics GSLs in a manner analogous to that observed in human cell lines. In this case, the glycosyl modification of the sphingolipid used (lac-Cer; galactos-β4-glucose-β-ceramide) is structurally very similar to that found on an endogenous fly glycolipid, mactosyl-ceramide (mannose-β4-glucose-β-ceramide). By carrying out time-course pulse-chase experiments with fluorescent BODIPY–lac-Cer on cells transfected with endolysosomal, Golgi, and recycling en-

This article was published online ahead of print in *MBC in Press* (http://www.molbiolcell.org/cgi/doi/10.1091/mbc.E09–01–0005) on January 6, 2010.

† These authors contributed equally to this work.

Author contributions: R.H., E.L., S.H., S.S., J.Y.L., and D.S.K.C. designed and carried out the experiments; N.E. synthesized the BODIPY-FR–lac-Cer; and R.K. conceived of the study, designed experiments, and wrote the manuscript.

Present addresses: *Institut für Bioverfahrenstechnik, Technische Universität München, 85748 Munich, Germany; §National Centre for Biological Sciences, GKVK, Bellary Road, Bangalore 560065, India; ‖Third Physikalisches Institut, University of Stuttgart, Pfaffenwaldring 5, D-70550 Stuttgart, Germany; #Cell Signaling and Developmental Biology, Department of Biological Sciences, The National University of Singapore, 14 Science Drive 4, Singapore 117543.

Address correspondence to: Rachel Kraut (rskraut@ntu.edu.sg).

Abbreviations used: AMPK, adenosine monophosphate–activated kinase; BODIPY, dipyrromethene boron difluoride; c6, DL-DmBG2-c6; FR, Far Red; GSL, glycosphingolipid; NPC, Niemann-Pick type C; lac-Cer, lactosyl ceramide; LAMP, lysosome-associated membrane protein; MannII-GFP, mannosidase-II-GFP; MβCD, methyl-β-cyclodextrin; M3-BPYE, *Drosophila* M3 medium with bacto-peptone and yeast extract.

dosomal markers, we establish that lac-Cer is less Golgi-localized than in mammalian fibroblasts and is found predominantly in recycling endosomes. Additionally, fluorescently tagged ceramide, which is thought to label exclusively Golgi in mammalian cells, traffics in part to endolysosomal vesicles.

In answer to the second aim of this study, whether sphingolipid trafficking in *Drosophila* is affected by cholesterol perturbations, we establish that cholesterol manipulations in neurons indeed influence the trafficking behavior of BODIPY–lac-Cer. After cholesterol overload, the effect is analogous to that which has been reported in the case of Niemann-Pick type C (NPC) fibroblasts, where lac-Cer accumulates aberrantly in an endolysosomal compartment (Pagano, 2003). Although mammalian studies were unable to assess changes in lac-Cer trafficking under cholesterol depletion, we find that cholesterol depletion causes an unexpectedly similar targeting of lac-Cer to endolysosomes, but also transiently increases it in Golgi.

Finally, we identify a novel phenomenon whereby fluorescent lac-Cer and an endocytic cargo dextran, which is normally targeted differently, influence each other's behavior and traffic together when both are present simultaneously at the membrane. We propose to call this phenomenon "hijacking" because it involves the rerouting of the trafficking of one label by the other.

In summary, we have found that glycosphingolipid trafficking in *Drosophila* neurons follows routes similar to that described in mammalian cells and importantly, that its behaviors are strongly influenced by conditions of cholesterol storage. These experiments constitute a first step in establishing a basis for studying the effects of lipid storage diseases and other neurodegenerative diseases on lipid trafficking, in the context of a genetically manipulable organism.

## MATERIALS AND METHODS

### *Cell Culture and Transfection*

Neuronal *Drosophila melanogaster* (DL-DmBG2-c6) cells were obtained from the *Drosophila* Genome Resource Center (DGRC, Bloomington, IN) and cultured at 25°C in Schneider's medium (Invitrogen, Carlsbad, CA) supplemented with 10% FBS (Invitrogen), 0.125 IU/ml insulin (Biological Industries, Beit Haemek, Israel) and 1% antibiotic/antimycotic solution (Invitrogen). Transfections of LAMP-green fluorescent protein (GFP), mannosidaseII (MannII)-GFP, and Rab11-GFP were carried out using CellFectin lipid reagent (Invitrogen) according to manufacturer's instructions.

### *Synthesis of BODIPY650/665–lac-Cer*

Far Red (FR) BODIPY650/665–lac-Cer was synthesized as follows:

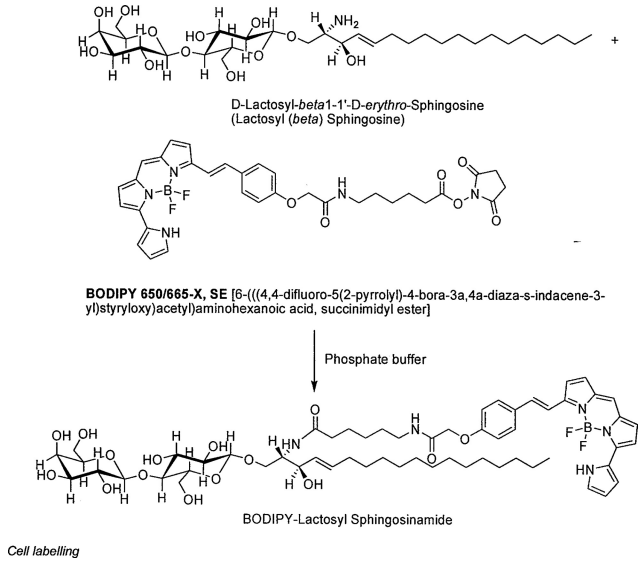


A flame-dried 5-ml reaction vial was charged with *D*-lactosyl-*beta*-1′-*D*-*erythro*-Sphingosine (4.87 mg, 0.0078 mmol; Avanti Polar Lipids, Alabaster, AL) and BODIPY 650/665-X (5 mg, 0.0078 mmol; Invitrogen) under argon atmosphere and was cooled in an ice bath at 0°C. Dry dimethyl formamide, 0.5 ml, was added dropwise and was stirred at 0°C for 2 h. The reaction mixture was allowed to come to room temperature and stirring continued for 24 h. The reaction was monitored by HPLC. After completion of the reaction, dimethyl formamide was removed under high vacuum, and the blue residue was purified by flash column chromatography using a Combiflash separating system (Teledyne Isco, Lincoln, NE). The desired fractions were collected and lyophilized to get the FR-BODIPY as a dark bluish green solid (8 mg, 89% yield), which was characterized by standard procedures. The obtained powder was subsequently complexed with defatted bovine serum albumin as described elsewhere (Martin and Pagano, 1994).

### *Cell Labeling*

BODIPY–lac-Cer and BODIPY–TR-Cer complexed to bovine serum albumin, and 10-kDa dextran–Alexa546 and –Alexa647 were from Molecular Probes (Eugene, OR). FL-BODIPY–lac-Cer, BODIPY650/665-lac-Cer, and BODIPY–TR-Cer were incubated on cells at 5 $\mu$M in Hanks' buffered salt solution (HBSS)/10 mM HEPES for 30 min at either 25°C or at 4°C for simultaneous labelings with 10-kDa dextran–Alexa488; FR-dextran (10-kDa dextran–Alexa647), and 10-kDa dextran-Alexa488 or 546 (all from Invitrogen) were incubated at 0.5 mg/ml for 5 min at 25°C. After labeling, cells were washed three to five times in HBSS/10 mM HEPES, followed by Schneider's medium, supplemented with 1% (vol/vol) OxyFluor (Oxyrase, Mansfield, OH), for imaging. FM1-43 and Hoechst dyes were used according to manufacturer's instructions.

### *TLC Analysis of Internalized BODIPY–lac-Cer*

C6 cells were incubated with 0.167 $\mu$M of BODIPY-FL–lac-Cer (C5; Invitrogen) for 30 min, washed, and further incubated in standard culture medium for 0, 6, and 14 h at 25°C. Lipids were extracted using standard protocols (Koval and Pagano, 1989) and run on TLC plates (Merck, Schwalbach, Germany) using the solvent methanol:choloroform:15 mM $CaCl_2$ in the ratio of 60:35:8 (vol/vol). Plates were first imaged with a GFP filter using an Explore Optix MX system (GE Healthcare, Munich, Germany). They were later exposed to iodine crystals to calculate the Rf (retention factor) values. Some standard lipids (Avanti Polar Lipids, Alabaster, AL) were also run on the TLC plates to estimate Rf values; they are as follows: BODIPY FL–lac-Cer (C5; Invitrogen) Rf = 0.59; lac-Cer (C12) Rf = 0.57; Cer (C17) Rf = 0.82; and GlcCer(C12) Rf = 0.67. The relative fluorescence intensity of a fluorescent metabolized product, visible as a second spot below intact BODIPY FL–lac-Cer was used to calculate the percentage breakdown.

### *Cholesterol Depletion and Overload*

For cholesterol depletion, mannosidaseII-GFP or LAMP-GFP–transfected cells were incubated with 10 mM methyl-$\beta$-cyclodextrin (M$\beta$CD; Sigma-Aldrich, Munich, Germany) at 25°C for 30 min in serum-free medium, before labeling. After labeling, cells were further incubated in serum-free medium. For cholesterol excess, 10 mM M$\beta$CD–cholesterol complexes were prepared as in Klein *et al.* (1995) and incubated with cells at 25°C for 30 min before labeling. After treatment cells were further incubated in complete medium with serum.

### *Inhibitor Treatments*

Inhibitors used were as follows: Dynasore, Chlorpromazine, and nystatin (Sigma-Aldrich). *Clostridium difficile* type B toxin (Merck) was prepared according to manufacturer's instructions, diluted in complete M3-BPYE cell culture medium, and applied at 25°C to cells.

C6 cells grown on eight-well glass chambers were treated with inhibitors as follows. Cells were treated with 25 $\mu$g/ml nystatin for 30 min, washed with HEPES/HBSS, and then pulse-labeled with fluorescent lipid in presence of nystatin. Samples were incubated with 5 $\mu$g/ml Chlorpromazine for 30 min and pulse-labeled with fluorescent lipid in the presence of Chlorpromazine. Samples were incubated with 4 ng/ml *C. difficile* toxin B for 2 h, washed with HEPES/HBSS, and then pulse-labeled with fluorescent lipid in presence of the drug. Cells were incubated with 60 $\mu$M Dynasore for 30 min, washed with HEPES/HBSS, and pulse-labeled with fluorescent lipid in the presence of dynasore in complete M3-BPYE (*Drosophila* M3 medium with bacto-peptone and yeast extract).

### *Microscopy and Postimaging Analysis*

Confocal microscopy was carried out using a Leica SP2 microscope with a 63×/0.9 NA water dipping lens (Heidelberg, Germany). For double-labeling experiments, control experiments were carried out using the single fluorophores, to verify that there was no cross-talk between the emission channels.

For colocalization experiments all images in a given experiment were taken and processed identically. Colocalization values were calculated for at least 15 cells at each time point, using the Costes algorithm (Costes *et al.*, 2004) that is available through ImageJ (rsb.info.nih.gov/ij) with the additional plugins: "Colocalization Test" and "Colocalization Threshold" (by T. Collins and W.

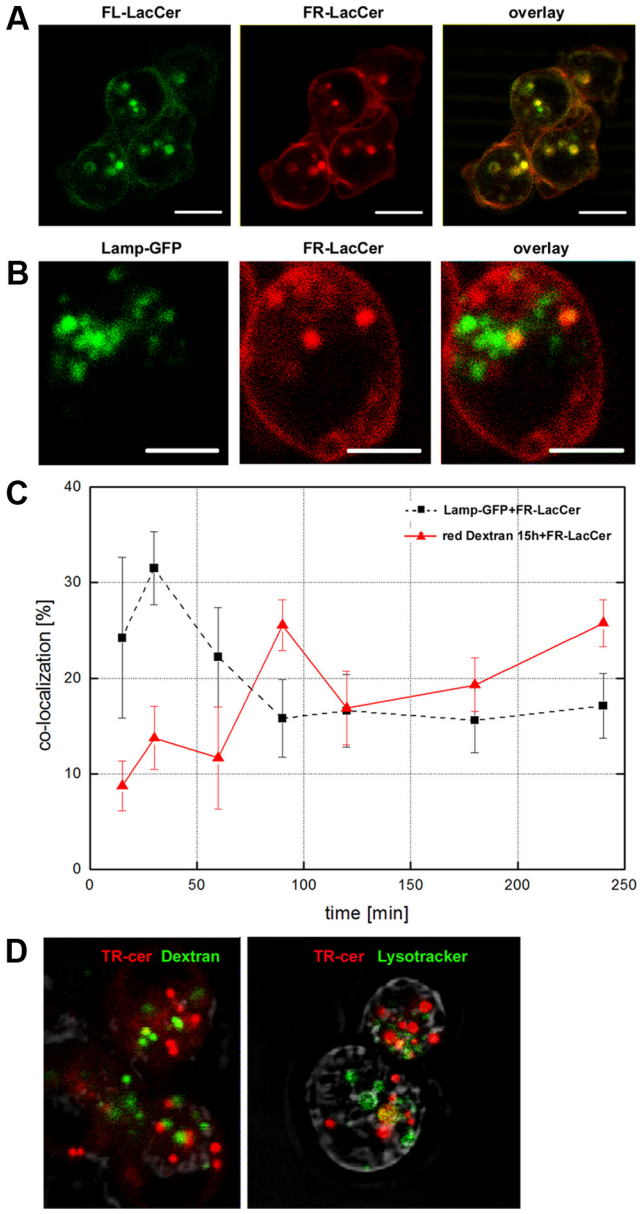


**Figure 1.** BODIPY-labeled lac-Cer analogs are taken up into endocytic vesicles in *Drosophila* neurons (A) BODIPY–lac-Cer is incorporated into the plasma membrane and endocytosed in *Drosophila* neurons incubated with a mixture of BODIPY FR-lac-Cer and FL-lac-Cer. The attached fluorophore (BODIPY 505-511 FL vs. BODIPY 650-665 FR) does not influence the uptake or subcellular trafficking of lac-Cer; the two labels traffic identically as can be seen by nearly complete overlap of the FL (green) and FR (red) signals. BODIPY–lac-Cer carrying compartments are highly mobile, typical for endosomes (see Supplemental Video1). Scale bar, 8 $\mu$m. (B) BODIPY-FR–lac-Cer (red) colocalization, with transfected lysosomal marker LAMP-GFP (green) after 30-min incubation at 4°C and subsequent chase at 25°C. Image shown is after 90 min. Scale bar, 5 $\mu$m. (C) Transfected LAMP-GFP and pulsed BODIPY-FR–lac-Cer colocalization (black trace) shows a peak in presumptive sorting endosomes at ~30 min after uptake, falling to ~15% at the sorting to late endosome transition (60–90 min). Red dextran was incubated on the cells for 5 min and chased for 15 h to label late endosomes and lysosomes. Note that colocalization with dextran (red trace) is not identical to that with LAMP-GFP. There is a transient peak in BODIPY-FR–lac-Cer colocalization with LAMP-GFP, versus the gradual increase in colocalization with dextran-positive lysosomes, presumably due to additional presence of the LAMP-GFP marker in sorting endosomes. (D) A nonglycosylated sphingolipid TR-ceramide (red) also colocalizes to a limited extent with the lysosomal markers dextran-Alexa488 (green) and Lysotracker-green that were incubated on the cells 3 h into the chase and imaged after 2 additional hours of chase (total chase time for TR-ceramide = 5 h; colocalization was not quantified).

Rasband) and "BG Subtraction from ROI" (by M.Cammer and T. Collins). The region of interest (ROI) was set such that plasma membrane staining was not analyzed.

For uptake experiments images were acquired with a CoolsnapHQ CCD camera (Photometrics, Woburn, MA) on a Deltavision (Applied Precision, Issaquah, WA) wide-field microscope with a 60×/1.42 NA oil lens (Olympus, Hamburg, Germany) and a standard (green ex490/20, em528/38; red ex555/28, em617/73) filter set (Chroma Technology, Brattleboro, VT). Quantification of images was performed with ImageJ. Uptake was determined by drawing borders around individual cells and counting spots after background (the intensity level between cells in a field) was subtracted. All photomicrographs in a given experiment were exposed and processed identically for a given fluorophore.

### *Primary Drosophila Neuronal Cultures*

Primary neurons were cultured by dissecting third instar larval brains in Schneider's culture medium containing antibiotic penicillin/streptomycin and washing in insect saline. Neurons were incubated in 0.5 mg/ml collagenase (Sigma-Aldrich) in insect saline for 30 min at room temperature and were gently washed in Schneider's medium with antibiotic before dissociation of the neurons by vortexing and pipetting up and down several times. The cell suspension from ~20 brains was pipetted in a volume of 20 $\mu$l per brain (400 $\mu$l) into four chambers of a multiwell imaging chamber with a coverslip bottom, which had been pretreated with poly-D-lysine, dried, and sterilized by UV irradiation. The neurons were allowed to adhere for ~2 h before labeling with dextran-Alexa488 in HBSS for 60 min, washing gently, and chasing overnight with full medium. BODIPY-FR–lac-Cer was added thereafter for 60 min in HBSS, washed gently, and chased for 3 h with full medium. Images were acquired using Metamorph software (Universal Imaging, West Chester, PA) on a wide-field fluorescence Zeiss Axiovert microscope at 100× magnification, 1.4 NA (Jena, Germany). Control strains Canton-S and *yw* and mutants in *löchrig* and elav-GAL4>EP-*Blue cheese* (n = 41 and 47, respectively) were used for primary neuronal cultures.

## RESULTS

### *LacCer Is Taken Up in an Endocytic Pathway by Drosophila Neurons*

We studied the uptake and trafficking of fluorescently labeled analogs of the simple GSL lac-Cer in the *Drosophila* larval brain-derived neuronal cell line DL-DmBG2-c6 (hereafter referred to as c6) (Ui *et al.*, 1994). Flies produce GSLs, but because their content and structure are different from mammalian GSLs (Seppo *et al.*, 2000), it was important to establish that mammalian-type GSLs could be incorporated, as they are in mammalian cells and that flies traffic these lipids in an analogous way. Fluorescent lac-Cer trafficking has been characterized as an indicator of GSL trafficking defects in human fibroblasts where cholesterol trafficking is disturbed (Puri *et al.*, 2001; Choudhury *et al.*, 2002, 2004; Sharma *et al.*, 2003; Singh *et al.*, 2003), and in fact, these two lipid classes are known to traffic interdependently (Sillence *et al.*, 2002; Puri *et al.*, 2003; Mukherjee and Maxfield, 2004; Sharma *et al.*, 2004; te Vruchte *et al.*, 2004).

As is the case in mammalian cells, exogenously applied analogs are taken up via the plasma membrane into endocytic vesicles by *Drosophila* c6 neurons (Figure 1, A and B). Fluorescent BODIPY-FL–tagged lac-Cer (BODIPY-FL–lac-Cer; Invitrogen) gradually becomes incorporated into mobile endocytic vesicles after 30-min incubation on the cells (shown after 1-h chase, Supplemental Video 1; video1.mp4) over ~10 min, from an initially uniform distribution at the plasma membrane. This behavior was observed for both BODIPY-FL–tagged lac-Cer, as well as a novel BODIPY-FR–

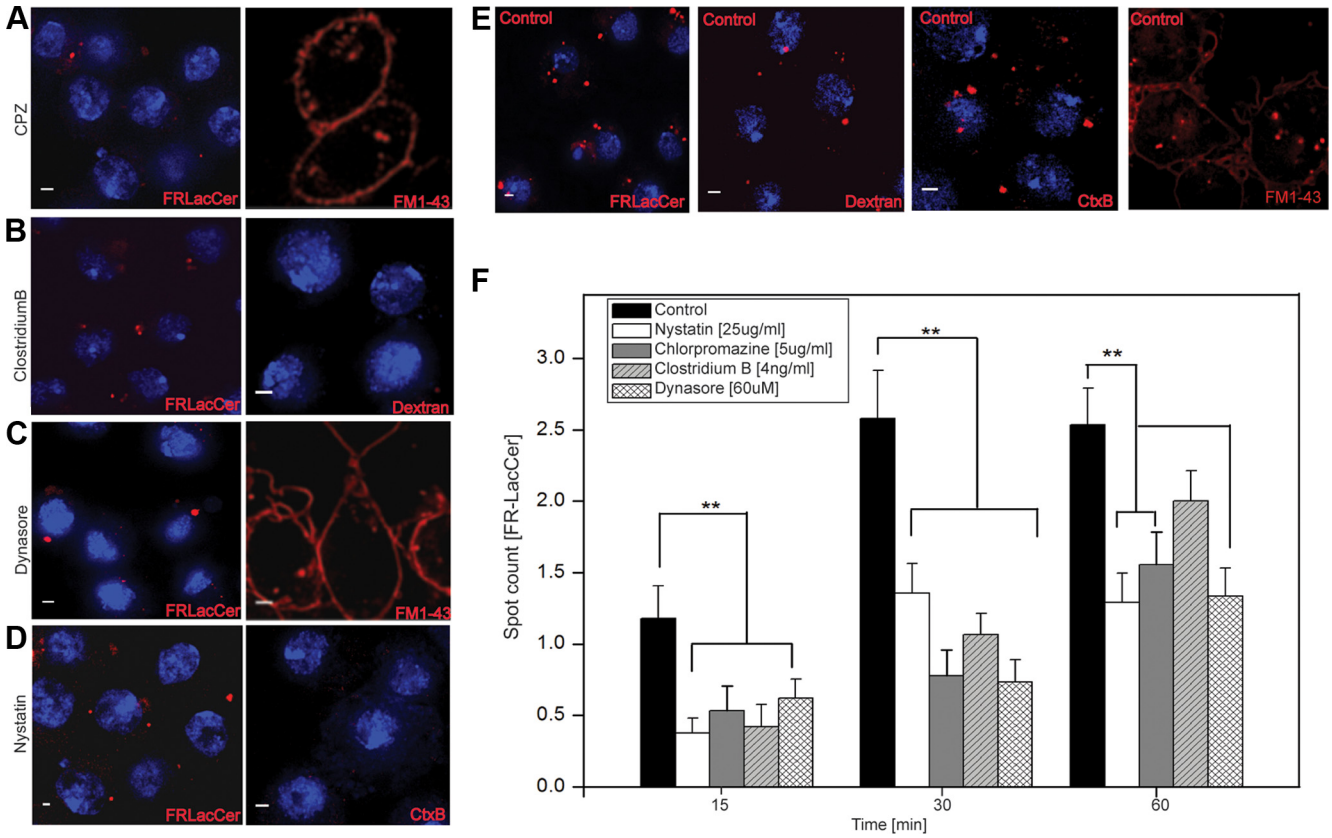


**Figure 2.** BODIPY–lac-Cer uptake is attenuated by inhibitors of both raft and nonraft endocytic mechanisms in fly neurons. (A–D) BODIPY-FR–lac-Cer (red), shown in far left column, compared with control probes (right column; blue) incubated with *Drosophila* c6 neurons treated with the given inhibitors: CPZ (chlorpromazine) inhibits clathrin-mediated uptake; *Clostridium* toxin B inhibits rho-family GTPases; dynasore inhibits dynamin; and nystatin inhibits cholesterol-dependent uptake. After imaging, cells were fixed and labeled with Hoechst dye (blue) to obtain images. (E) Uptake of the different labels in untreated control cells, for comparison (not quantified). (F) Quantification of uptake by spot count (see *Materals and Methods*) at various time points after labeling with FR–lac-Cer. nystatin, dynasore, and chlorpromazine (white, gray, and cross-hatched bars) exerted more long-lasting inhibition on uptake than *Clostridium* toxin B (single cross-hatch), which gave close to complete recovery by 60 min. Significant differences; ***$p < 0.01$).

tagged lac-Cer (see *Materials and Methods*), and these two analogs colocalized nearly completely (Figure 1A), indicating that the choice of fluorophore does not influence the uptake or subcellular trafficking of lac-Cer.

BODIPY-FR–lac-Cer colocalizes with LAMP-GFP (Pulipparacharuvil *et al.*, 2005) at a peak value of $tM_{lac\text{-}Cer} \approx 30\%$ after 30 min of chase time (Figure 1C); colocalization was calculated using the Manders algorithm with Costes thresholding (Manders *et al.*, 1993; Costes *et al.*, 2004). At this time, a fluid-phase marker of endocytic uptake, 10-kDa dextran, passes through the sorting endosomal compartment (Sriram *et al.*, 2003). LAMP-GFP, although ostensibly a lysosomal marker, is also partially distributed in earlier, highly mobile endosomal compartments (R.K., unpublished observations), some of which may be mildly acidified (pH 5.9–6) sorting endosomes (Hunziker and Geuze, 1996; Steinert *et al.*, 2008). After the 30-min peak, colocalization with LAMP-GFP fell over the next hour to ~15%, when dextran at a similar time would be exiting the sorting endosome and entering the late endosomal portion of the pathway (Sriram *et al.*, 2003). Thereafter, colocalization remained constant at ~15% for up to 4 h of chase (Figure 1, B and C). Therefore, we conclude that BODIPY–lac-Cer transiently passes through sorting endosomes at ~30 min en route to other compartments.

As a comparison to the colocalization of BODIPY-FR–lac-Cer with LAMP-GFP, dextran-Alexa594 was chased in the cells overnight to label late endosomes/lysosomes, and these cells were then labeled with BODIPY-FR–lac-Cer and imaged after the given chase times (Figure 1C), Initial colocalization is lower than with LAMP-GFP, and the peak in presumptive sorting endosomes is absent (compare red dextran trace to black LAMP-GFP trace) but increases to ~20% after 90 min.

We also observed that a nonglycosylated fluorescent sphingolipid, FL-BODIPY- or TR-BODIPY-ceramide (FL- or TR-Cer), is taken up into mobile endosomes as is the glycosylated BODIPY–lac-Cer and exhibits the interesting property of trafficking in tubulovesicular compartments that move along the length of neuronal processes (see Supplemental Video 2). TR-Cer also showed some colocalization with dextran-Alexa488 and lysotracker-green, which were added after the TR-cer labeling, although this was not quantified (Figure 1D).

### *BODIPY–lac-Cer Uptake Is Sensitive to Inhibitors of Cholesterol- and Dynamin-mediated Endocytosis*

To discover the mechanism of BODIPY–lac-Cer uptake into *Drosophila* neurons, cells were treated with pharmacological inhibitors of different uptake mediators, then incubated with BODIPY–lac-Cer or control labels, and chased in the presence of the drug. Figure 2 shows an uptake time course, where the number of internalized vesicles containing

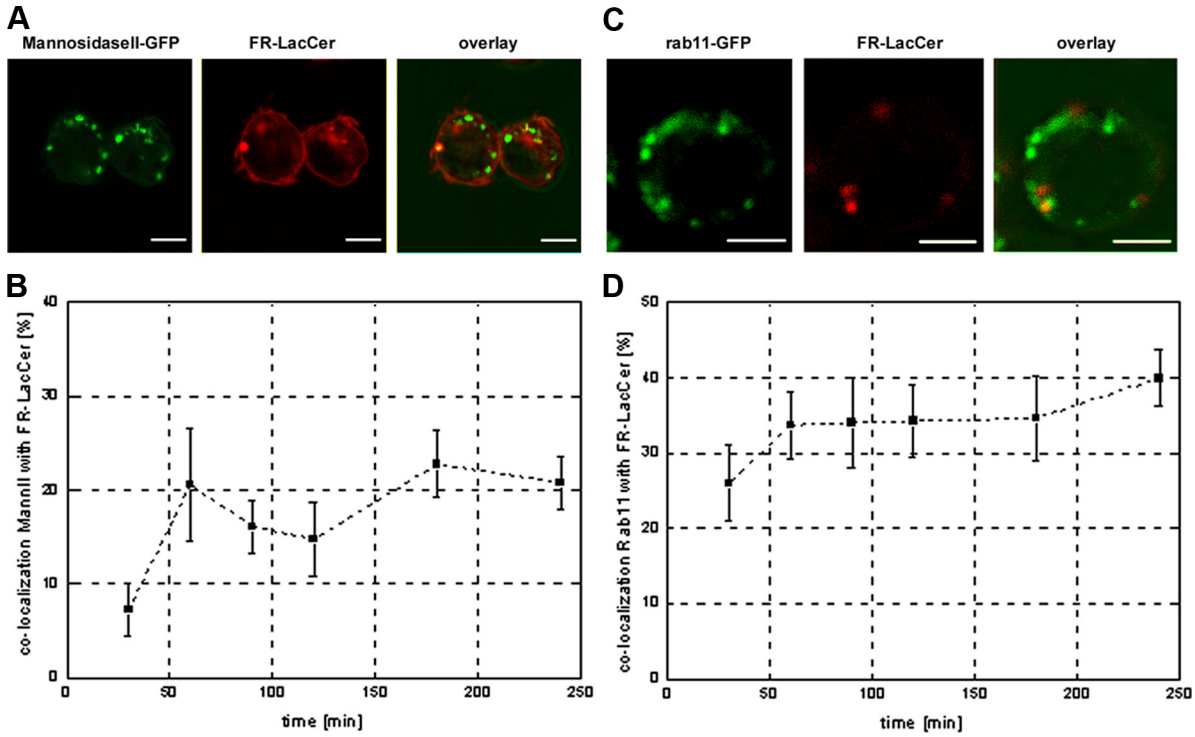


**Figure 3.** BODIPY–lac-Cer traffics primarily through recycling endosomes and is only partially Golgi-associated. (A and B) BODIPY–lac-Cer (red) colocalization with transfected MannII-GFP (green). After 60 min, BODIPY-FR–lac-Cer traffics only partially (~15–20%) to *cis* and medial Golgi compartments, labeled by MannII-GFP. Bars, 5 $\mu$m. (C and D) BODIPY–lac-Cer– (red) colocalization with rab11-GFP– (green) positive recycling endosomes. Trafficking of BODIPY-FR–lac-Cer (35–40%) to recycling endosomes is substantially higher than that to Golgi. Scale bars, 4 $\mu$m.

BODIPY–lac-Cer is quantified (see *Materials and Methods*) at different times after chase. Inhibition of clathrin-mediated uptake by chlorpromazine (Figure 2, A and F) also inhibits BODIPY–lac-Cer uptake substantially, but this recovers to some extent after 1 h. FM1-43 uptake is not strongly affected (Figure 2A).

To distinguish between rho-family GTPase-mediated uptake versus dynamin-mediated uptake of BODIPY–lac-Cer in fly neurons, the rho-family GTPase inhibitor *Clostridium* type B toxin and the dynamin inhibitor Dynasore (Macia *et al.*, 2006) were applied. Inhibition of rho-mediated uptake by *Clostridium* B toxin (Puri *et al.*, 2001), similar to clathrin uptake, lowered BODIPY–lac-Cer uptake initially (Figure 2B), but this also recovered to nearly normal levels after 60 min. As expected, uptake of dextran-Alexa594, which in mammalian cells is mediated by rho family member cdc42, was strongly inhibited compared with the control (Figure 2B). Dynasore inhibited uptake of BODIPY–lac-Cer throughout the time course (Figure 2, C and F).

Finally, nystatin was used as an inhibitor of raft-mediated uptake by virtue of its cholesterol-extracting properties (Puri *et al.*, 2001). This was as effective as Dynasore in continuously inhibiting BODIPY–lac-Cer uptake throughout the time course and also inhibited CtxB uptake compared with control (Figure 2, D–F). Apparently unlike mammalian fibroblasts, however, where lac-Cer uptake is completely inhibited by raft- and dynamin inhibitors, but completely unaffected by clathrin inhibitors (Puri *et al.*, 2001), the inhibition of fluorescent lac-Cer uptake in fly neurons is only partial.

The inhibitor studies in summary suggest that although BODIPY–lac-Cer uptake can be perturbed by interference with several different uptake pathways (including clathrin- and rho-family mediated), the effect of dynamin inhibition is stronger than that of the rho family inhibitor, similar to the case in mammalian cells (Puri *et al.*, 2001). As in mammalian cells, nystatin also effectively inhibited uptake, indicating that a cholesterol-mediated mechanism, and therefore a possible association with lipid rafts, is at least in part responsible for uptake.

### *Lac Cer Is Only Partially Golgi Associated*

Because BODIPY–lac-Cer had been characterized as traversing the Golgi in human fibroblasts, we tested for colocalization between BODIPY–lac-Cer and the transfected *Drosophila* Golgi marker MannII-GFP (Bard *et al.*, 2006; Figure 3, A and B). Starting from <10% colocalization at 30 min, colocalization increased to 20% at 1 h, and thereafter hovered near 20% for up to 4 h (Figure 3B). This is significantly lower than would be expected for an exclusively Golgi marker. To eliminate the possibility that some of the fluorescent lac-Cer was being metabolized into other products, which might localize differently, the labeled cells were extracted, and the lipids were analyzed by TLC. After 6 h of chase, all of the BODIPY–lac-Cer was still present (see *Materials and Methods* and Supplementary Figure S3). Only after 14 h of incubation, fluorescence intensity quantification of the two spots indicated that an average of 16.5% of BODIPY–lac-Cer had been metabolized to other products.

Previously, it was reported that lac-Cer is partially trafficked to the Golgi compartment, with a minor early contribution from recycling endosomes, which cycle the lipid back to the plasma membrane (Sharma *et al.*, 2003). Given the relatively low degree of BODIPY–lac-Cer trafficking to the

Golgi and endolysosomal compartments in our cell line (each only ~20%; Figures 1, B and C, and 3, A and B), we tested for its presence in other compartments. We found that a substantial portion (35–40%) of BODIPY–lac-Cer trafficked to rab11-GFP–labeled recycling endosomes (the rab11-GFP plasmid was a kind gift of H. Chang [Purdue University]; Figure 3, C and D). Sharma *et al.* (2003) also report a contribution from the recycling endosome to BODIPY–lac-Cer's distribution in fibroblasts, but in their report this dropped rapidly (after 15 min) because the label was recycled back to the plasma membrane. BODIPY–lac-Cer in the fly cells trafficked primarily to recycling endosomes, and about half as much was found in Golgi over an extended time period, but no major loss of the label was noted.

From our quantitative time-course colocalization studies, it appears that after passing through sorting endosomes, BODIPY–lac-Cer is present primarily in the recycling endosomal compartment, and the remainder is localized to the Golgi and to lysosomes. A small proportion remains in LAMP-GFP–positive vesicles that we presume to be sorting endosomes. This is similar to what was reported in fibroblasts (Puri *et al.,* 2001; Sharma *et al.,* 2003), but our study's findings differ in that the Golgi contribution is much less than that of recycling endosomes.

### *BODIPY–lac-Cer Can Hijack the Trafficking Route of an Endocytic Cargo*

Earlier studies by Pagano and coworkers showed that lac-Cer stimulates caveolar uptake from the plasma membrane (Sharma *et al.,* 2004). Our experiments reveal a novel effect, distinct from simple stimulation of uptake, whereby lac-Cer and another endocytic cargo, dextran, exert a mutual influence on each other's trafficking routes. Rerouting through a novel pathway would not be expected if lac-Cer were merely stimulating endocytosis, and carried dextran with it.

In mammalian cells, lac-Cer and dextran are taken up via different endocytic pathways that depend on different accessory proteins (dynamin vs. cdc42), and are inhibited by different drugs (Puri *et al.,* 2001; Sharma *et al.,* 2003; Singh *et al.,* 2003). Similarly, in *Drosophila* cells BODIPY–lac-Cer and dextran trafficking is almost entirely separate when incubated independently (Figure 4), but surprisingly, they show almost complete colocalization when incubated directly one after the other.

Sequential labeling of BODIPY-FL–lac-Cer and then FR-dextran (lac-Cer pulse, 3-h chase, dextran pulse, 2-h chase) or conversely, dextran and then BODIPY-FL–lac-Cer (dextran pulse, 2-h chase, lac-Cer pulse, 3-h chase) both resulted in nearly no colocalization (Figure 4, B and D). This was expected, because after 5 h BODIPY lac-Cer is not targeted primarily to lysosomes (see Figure 1; Puri *et al.,* 2001), whereas dextran is predominantly lysosomal. Unexpectedly, however, BODIPY–lac-Cer and dextran traffic completely together when added simultaneously (the thresholded Manders' coefficient [tM] ≈ 80%; Figure 4, A and C). This is not likely to be due to direct binding between the two labels, because the BODIPY–lac-Cer is washed out briefly before addition of the dextran, and the same effect was seen when the relative amounts of the two labels were varied (Figure 4E). The effect of BODIPY–lac-Cer on the trafficking of other cargoes appears not to be limited to insect cells, because a similar effect was observed in mammalian SH-SY5Y neuroblastoma (Figure S4), where dextran incubated with BODIPY–lac-Cer simultaneously colocalized to a greater extent than when the two were incubated sequentially and chased for long enough to reach their final destinations. $tM_{dextran}$ was 0.4 ± 0.021 when incubated sequentially, versus 0.67 ± 0.015 when incubated simultaneously ($p = 3.24226E-11$).

We wanted to find out more about the mechanism of this rerouting phenomenon and whether the new trafficking route was more like BODIPY–lac-Cer, or dextran, or a hybrid. To characterize the new routes of the BODIPY–lac-Cer + dextran combination in *Drosophila* neurons, we carried out time-course colocalizations with BODIPY–lac-Cer + dextran in the presence of either a Golgi or a lysosomal reference marker and calculated colocalization of total BODIPY–lac-Cer intensity with the reference marker ($tM_{lac\text{-}Cer}$; Figure 5). In each case, BODIPY–lac-Cer colocalized completely with pulsed dextran (as seen in Figure 4A), but comparison with LAMP-GFP showed that BODIPY–lac-Cer diverted dextran away from endolysosomes (cf. green line with dashed black line; Figure 5A). Comparison with dextran incubated overnight to label lysosomes showed an even stronger diversion of the pulsed dextran away from lysosomes (compare green line with dashed black line; Figure 5B). The difference between the colocalization curves with LAMP-GFP versus overnight dextran is not unexpected, because LAMP-GFP is not strictly confined to lysosomes, as discussed earlier, and these two ostensibly lysosomal labels colocalize only ~40% with each other (Figure 4C).

BODIPY–lac-Cer's own itinerary is also slightly altered in the presence of dextran (cf. red lines with dashed black lines in Figure 5, A–C). In particular, BODIPY–lac-Cer + dextran follows a slower route toward the Golgi than BODIPY–lac-Cer alone (Figure 5C). BODIPY–lac-Cer + dextran appears to arrive late and persist at a slightly higher than normal level in endolysosomes labeled with LAMP-GFP (Figure 5A), whereas it is suppressed in lysosomes labeled with dextran overnight (Figure 5B). However, these changes in BODIPY–lac-Cer's trafficking behavior are not as drastic as those in dextran's pathway.

We conclude that BODIPY–lac-Cer interacting with a ligand may direct that ligand to an alternate intracellular path. Specifically, dextran, which ordinarily follows an endosome→late endosome→lysosome pathway, is rerouted completely away from late endolysosomes when BODIPY–lac-Cer is also present. We propose to call this phenomenon hijacking because it involves the rerouting of the trafficking of one agent by the other.

To test whether the uptake mechanism of the dextran is altered by BODIPY–lac-Cer as well as its trafficking route, we treated cells with inhibitors of dextran's and lac-Cer's uptake, as in Figure 2, and compared the degree of inhibition in the presence or absence of the other label (Figure 5, D–F). The colocalization between BODIPY–lac-Cer and dextran added together in the presence of inhibitors was also measured and was found to be still much higher than normal (i.e., sequential), although not as high as without the inhibitors (Figure 5D). This shows that even in the presence of one inhibitor or the other, the uptake of BODIPY–lac-Cer and dextran do not completely uncouple when they are both present at the membrane simultaneously. Images of cells incubated with both labels and the inhibitors are shown in Figure 5F.

*Clostridium* B toxin treatment of BODIPY–lac-Cer + dextran together showed that the uptake pathway of dextran is altered by the presence of the BODIPY–lac-Cer, because the inhibition is not as severe when BODIPY–lac-Cer is there (Figure 5E, left, dextran graph). In contrast, dynasore's effect on BODIPY–lac-Cer is just as inhibitory whether or not dextran is present (Figure 5E, right, BODIPY–lac-Cer graph).

Together, these experiments suggest that the uptake mechanism of dextran can be altered to a certain extent by lac-Cer present simultaneously at the membrane and that

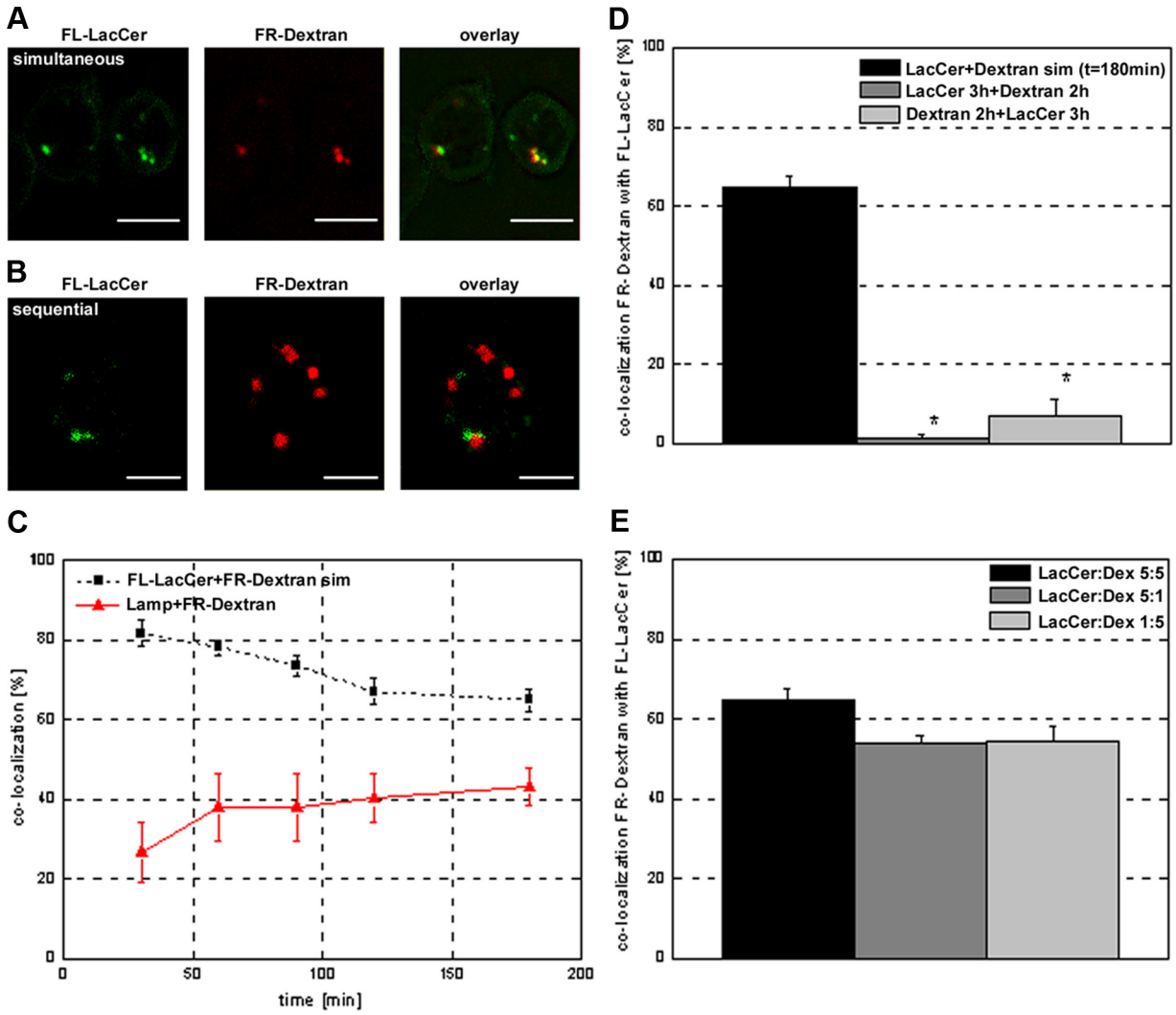


**Figure 4.** BODIPY–lac-Cer and dextran traffic identically when present simultaneously on cells. (A and B) Simultaneous labeling of BODIPY-FL–lac-Cer (green) with Alexa647 (FR)-dextran (red) resulted in very high colocalization. In contrast, sequential labeling of FL–lac-Cer and 3 h later with dextran results in essentially no colocalization between the two dyes, even given sufficient chasing time that each label by itself would have reached late endosomes or lysosomes. Bars, 8 $\mu$m. (C) Colocalization values are continuously high over time after simultaneous incubation of BODIPY–lac-Cer and dextran (black trace), even compared with that seen between dextran and another endolysosomal marker, LAMP-GFP (red trace; see Figure 1); "simultaneous" refers to addition of dextran immediately after brief washing of the BODIPY-FL–lac-Cer. (D) Colocalization after 3 h is high (>60%) when dextran and BODIPY–lac-Cer are simultaneously incubated (sim) and significantly lower when sequentially incubated, independent of the order of addition (dark and light gray bars). A failure to colocalize even after several hours indicates that BODIPY–lac-Cer and dextran are trafficked to different targets. Student's *t* test was used to compare the datasets from simultaneous versus sequential incubation; *$p < 0.05$. (E) BODIPY–lac-Cer influences trafficking of dextran independent of the relative concentrations of both dyes, indicating that the altered transport is not due to direct binding. Cells were incubated with 5 $\mu$M BODIPY-FL–lac-Cer and 0.5 mg/ml Alexa647-dextran (5:5), 5 $\mu$M BODIPY-FL–lac-Cer and 0.1 mg/ml dextran (5:1) and 1 $\mu$M BODIPY-FL–lac-Cer and 0.5 mg/ml dextran (1:5) simultaneously and colocalization values were calculated after 180 min.

the subsequent trafficking of dextran is strongly shifted by lac-Cer toward a nonlysosomal target.

### *BODIPY–lac-Cer Trafficking to Golgi versus Lysosomes Is Controlled by a Cholesterol Switch*

Pagano and colleagues have characterized changes in GSL trafficking in human fibroblasts as a cell culture model for lipid storage diseases, in particular NPC (Pagano, 2003). Under conditions of aberrant endolysosomal cholesterol storage brought about by the disease, BODIPY–lac-Cer accumulated in late endolysosomal compartments and was diverted from its normal Golgi itinerary (Choudhury *et al.*, 2002, 2004). Similarly, aberrant trafficking of GSL to lysosomes was found in a model of Gaucher disease (Sillence *et al.*, 2002). Therefore, it was important for us to address whether trafficking of GSLs in fly neurons is affected similarly to that in diseased human cells, under analogous conditions of lipid storage.

When cells are overloaded with cholesterol (see *Materals and Methods*), trafficking to endolysosomes is strongly increased at the expense of Golgi-directed trafficking (cf. blue trace to black trace, Figure 6, A and D). The initial uptake pathway, presumably through early and sorting endosomes, is not perturbed (Figure 6D, up to 60 min), but becomes noncoincident at the point of divergence between the Golgi and endolysosomal pathways (60–90 min).

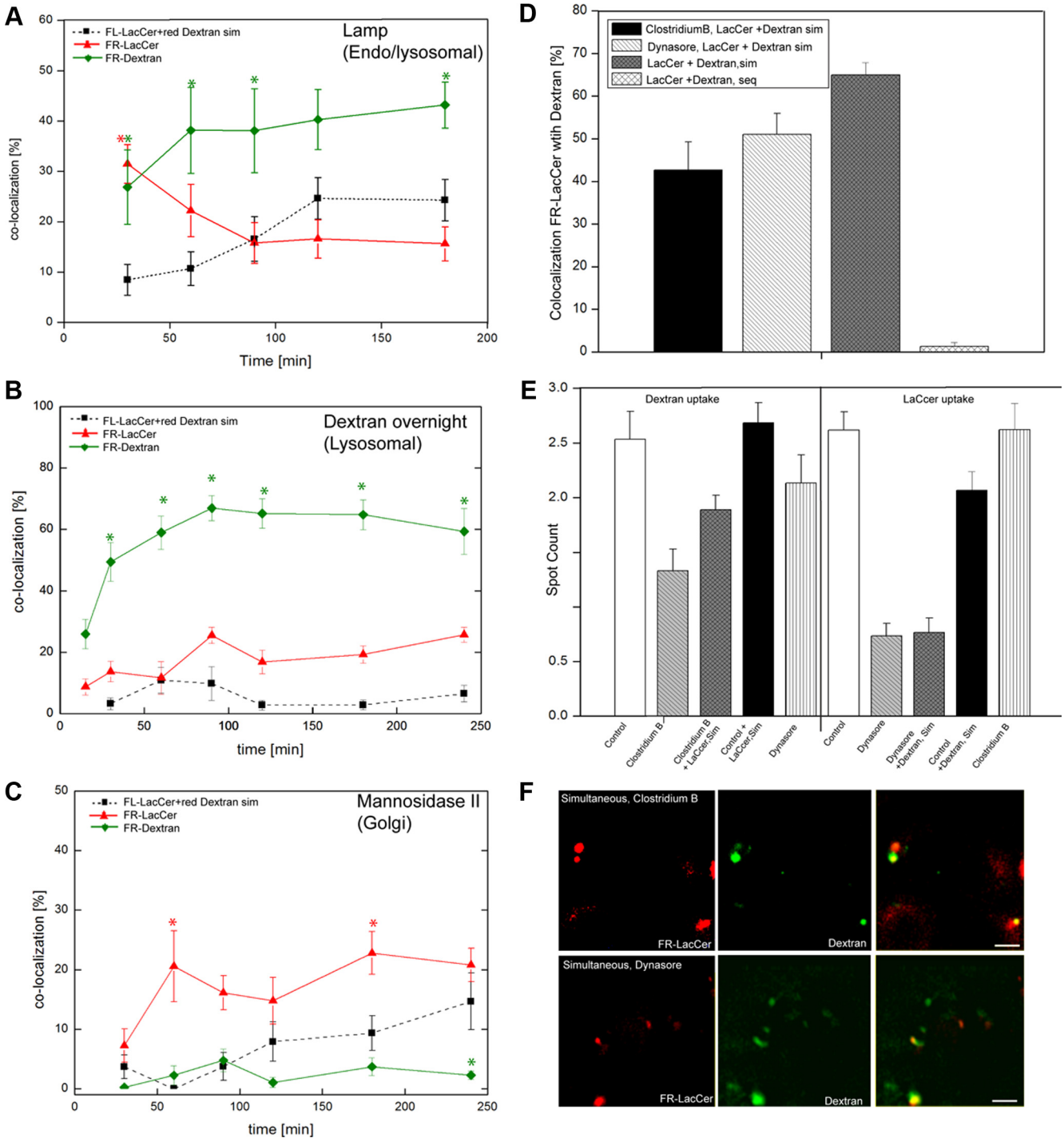


**Figure 5.** BODIPY–lac-Cer uptake in the presence of dextran alters trafficking itineraries of both tracers. Endolysosomes, Golgi, and lysosomes were labeled with LAMP-GFP (A), Alexa546-dextran (B), and MannII-GFP, chased for 15 h (C), and subsequently labeled with BODIPY-FL–lac-Cer and Alexa647-dextran simultaneously to determine whether the trafficking route of either label changed in the presence of the other. (A) After simultaneous incubation, both labels accumulate slowly in LAMP-positive compartments (black trace), more than would be expected for BODIPY–lac-Cer (red line), but less than dextran by itself (green line). (B) Trafficking of FR-dextran to lysosomes labeled by 15-h incubation of Alexa546-dextran (green line) was completely inhibited in the presence of BODIPY–lac-Cer (black trace). (C) Trafficking of BODIPY–lac-Cer to Golgi (normally ~20%; red line) is also inhibited by the presence of dextran (black trace). dextran does not normally traverse the Golgi in the absence of BODIPY–lac-Cer (green line). Significant differences in colocalization at given time points; *$p < 0.05$. (D) Quantification of colocalization of BODIPY-FR–lac-Cer with dextran added simultaneously, in the presence or absence of the inhibitor *Clostridium* toxin B (black), which affects dextran uptake (see Figure 1), and dynasore (light gray), which affects BODIPY–lac-Cer uptake. Colocalization remains nearly as high as after the control simultaneous incubation (dark gray) and much higher than after sequential incubation (hatched). (E, left) Quantification of dextran-Alexa488 uptake efficiency after 90 min, either alone (white) or together with BODIPY-FR–lac-Cer (black) in untreated cells, versus lower uptake in *Clostridium* toxin B–treated cells (gray). Uptake inhibition of dextran is rescued to an intermediate level by the presence of BODIPY–lac-Cer (dark gray hatched). Uptake of dextran alone is not

Under conditions of cholesterol depletion by incubation with MβCD, the converse effect is observed, with respect to Golgi trafficking: BODIPY–lac-Cer trafficking to Golgi appears to be initially slower than normal, until 2 h, and then shows an enhanced peak at 3 h (Figure 6A), which returns to a similar baseline as in the control cells after extended chase (4 h). The effectiveness of the cholesterol depletion and overload treatments were tested by quantifying sterol levels using the Amplex Red assay (Invitrogen), which showed that extracts of MβCD-treated c6 neurons had a 47 ± 8% reduction of cholesterol, and cholesterol-overloaded cells showed an increase of 250 ± 13% (Hebbar *et al.,* 2008). In Figure 9 of Steinert *et al.* (2008) we also showed that cholesterol-loaded c6 neurons labeled much more strongly with filipin, confirming the presence of excess free cholesterol. Here, representative images of cells that were treated and labeled with the different markers and BODIPY–lac-Cer (Figure 6, B–I) suggest that the observed changes in BODIPY–lac-Cer trafficking were not a result of less effective uptake due to cholesterol depletion or overload. However, the morphology of the endolysosomal compartments did seem to be altered under cholesterol loading (e.g., Figure 6F).

We were surprised to find that cholesterol depletion increased BODIPY–lac-Cer trafficking to endolysosomes to a similar degree as cholesterol excess late in the pathway (after ~90 min), with total colocalization for both being around 50% after 3 h, versus only 15% in untreated controls (Figure 6D). Colocalization of BODIPY–lac-Cer with the recycling compartment labeled with rab11-GFP was also monitored under both cholesterol excess and depletion, to find out whether the ectopic BODIPY–lac-Cer found especially in endolysosomes under both these conditions was being diverted from recycling endosomes (Figure 6G). Ordinarily, a large portion (~40%) of BODIPY–lac-Cer targets to the recycling compartment. Under cholesterol depletion, trafficking to recycling endosomes was almost eradicated, presumably going instead to sorting and then Golgi vesicles, in turn (red trace, cf. Figure 6, G with A and D; summarized schematically in Figure 7). It was also reduced gradually by ~10–15% under cholesterol excess, perhaps due to the slower accumulation of BODIPY–lac-Cer in late endolysosomes with cholesterol excess (cf. blue trace, Figure 6G,D; indicated by a dotted arrow in Figure 7).

To demonstrate the applicability of this method to actual *Drosophila* genetic models, we applied the same probes, BODIPY–lac-Cer and dextran, to primary cultured neurons from third instar larval brains of different control strains, versus genetic conditions that might be expected to alter lipid metabolism and/or storage. We tested mutants in the AMP-activated protein kinase (AMPK) gamma subunit *löchrig*, which are neurodegenerative and accumulate abnormally high levels of free sterol in the brain (Tschäpe *et al.,* 2002), as well as animals overexpressing the presumptive lysosomal/autophagic trafficking protein Blue cheese (Finley *et al.,* 2003; Simonsen *et al.,* 2007; Lim and Kraut, 2009) in the nervous system. Overexpression of Blue cheese in neurons results in abnormally high levels of sterol-ester and higher sterol levels overall in the adult brain (our unpublished observations). BODIPY–lac-Cer was found to be taken up readily by these neurons, and the degree of colocalization of BODIPY–lac-Cer with fluorescent dextran-Alexa488 that had been pulsed and chased overnight was measured after live pulse-chase experiments similar to those described in Figure 6 (see *Materals and Methods*). A comparison of neurons from larval brains of *yw* and *elav*-GAL4 strains as controls, with neurons from *löchrig* and *elav>blue cheese* brains suggested that there may be slightly greater trafficking of the sphingolipid analogue to degradative compartments in these neurodegenerative situations, although colocalization levels in general were higher than in the c6 cell line. Colocalization of BODIPY–lac-Cer with dextran-Alexa488 in the control neurons ranged from about $tM_{lac\text{-}Cer}$ ~ 0.51 to ~0.63. Primary neurons from *löchrig* and *elav>*EP-*blue cheese* animals had higher colocalization levels than *yw* ($tM_{lac\text{-}Cer}$ 0.68 and 0.70, vs. 0.51 respectively), but the differences between these and the *elav*-GAL4 controls were not as great (Figure S5). Altering lipid conditions in the culture medium and higher-resolution imaging methods will be tested as possible approaches to examine more closely what are now detectable as only subtle trafficking differences.

**Figure 5 (cont).** significantly inhibited by dynasore (light gray). (E, right) Quantification of BODIPY-FR–lac-Cer uptake efficiency after 90 min, either alone in untreated cells (white) or together with dextran (black), versus lower uptake in dynasore-treated cells (gray). Uptake inhibition is not rescued by the presence of dextran (dark gray hatched), in contrast to the situation on the left. Uptake of BODIPY-FR–lac-Cer alone is not inhibited by *Clostridium* toxin B (light gray). (F) Images of cells showing that the presence of inhibitors does not prevent colocalization of the two labels: BODIPY-FR–lac-Cer (red) and dextran (green).

## DISCUSSION

In this report, we have carried out the first characterization of the intracellular trafficking behavior of a simple glycolipid, lac-Cer, in *Drosophila* cells. Using systematic, quantitative time-course colocalizations and pharmacological inhibition, we have shown that a fluorescent glycolipid analog, BODIPY-FR–lac-Cer, is endocytosed primarily by a cholesterol- and dynamin-mediated mechanism and traffics between the biosynthetic (Golgi) and degradative (endolysosomal) pathways, with a major component (~40%) traveling through recycling endosomes. The trafficking switch between biosynthetic and degradative pathways appears to depend on free cholesterol levels in a manner similar to what was seen in mammalian cells (Puri *et al.,* 2001).

Because the composition of *Drosophila* sphingolipids and glycolipids is somewhat different from those of mammals, it was not obvious that this sphingolipid would behave in an analogous manner to that in the mammalian system. Fly sphingolipids, as well as their membrane lipids in general, have shorter acyl chains (a C14 sphingoid chain instead of the more common C18 in mammals; Holthuis *et al.,* 2001). Glycosphingolipids in fly contain mannose not galactose as the second sugar moiety (Wiegandt, 1992) and are not sialylated but instead contain phosphoethanolamine substituted *N*-acetyl-glucosamine (GlcNAc; Seppo *et al.,* 2000). In spite of these differences, our findings rather surprisingly support an overall conservation of the behavior of at least one simple two-sugar glycosphingolipid, lac-Cer. This may be because of the structural similarity between lac-Cer and the *Drosophila* equivalent mactosyl-cer, which besides the acyl chain length differs only in the orientation of one hydroxyl group on the terminal hexose (Seppo *et al.,* 2000).

### *The Intracellular Pathway and Sterol-dependent Uptake of lac-Cer in Drosophila is Similar to Mammalian Cells*

Although the overall intracellular distribution BODIPY–lac-Cer was conserved in *Drosophila* neurons, we found a stronger contribution from the recycling and lysosomal compartments than from the Golgi compared with what was previ-

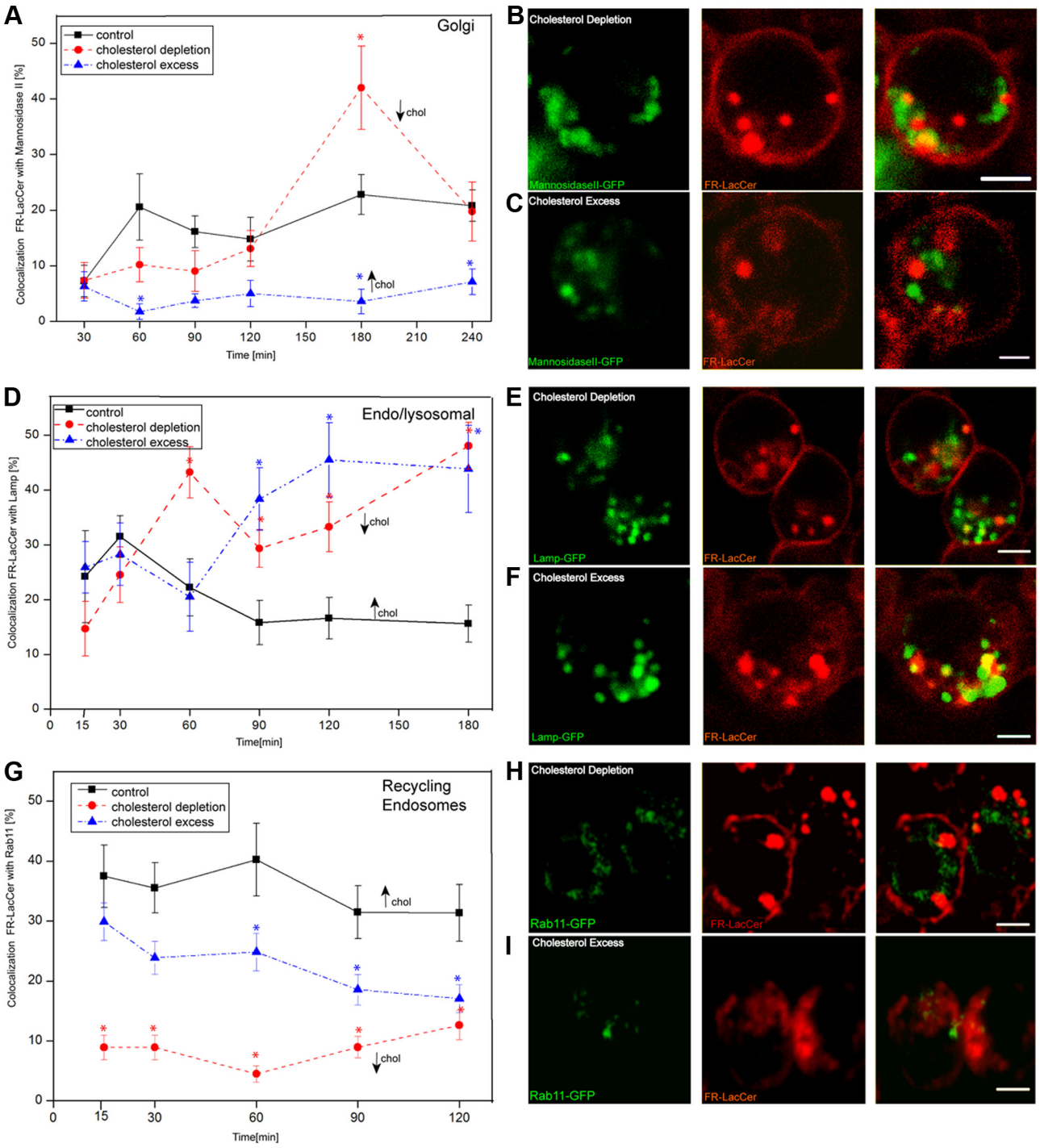


**Figure 6.** BODIPY–lac-Cer trafficking between Golgi, recycling endosomes, and the endolysosomal pathway is controlled by a cholesterol switch in fly neurons. (A, D, and G) Cholesterol depletion (red trace in all graphs). Loss of cholesterol leads to increased traffic through a LAMP-positive sorting compartment at 60 min (D) and then a significant but transient accumulation in Golgi labeled by MannII-GFP (A) at 180 min. BODIPY–lac-Cer finally accumulates in LAMP-positive late endolysosomes. Passage of BODIPY–lac-Cer through recycling endosomes in contrast is much reduced (G). The drop in Golgi at 240 min is probably not due to production of noncolocalizing metabolites of BODPIY-lac-Cer, because labeled lac-Cer remains stable for at least 6 h (see Supplemental Figure 3). Cholesterol excess (blue traces in all graphs): Cholesterol overloading strongly suppresses Golgi-targeting (A), in contrast to the enhancement of Golgi targeting seen under cholesterol depletion (red trace, A), and leads to aberrant accumulation in enlarged LAMP-positive (D) compartments, but with a later time course than depletion (compare blue and red traces, D). Colocalization is expressed as $tM_{lac\text{-}Cer}$, converted to %. Significance of the differences in colocalization; *$p < 0.05$. (B, C, E, F, H, and I) Images of c6 neurons transfected with markers of the different compartments and depleted or loaded with cholesterol: Golgi (MannII-GFP in B and C), endolysosomes (LAMP-GFP in E and F), and recycling endosomes (rab11-GFP in H and I; all green), and labeled with BODIPY-FR–lac-Cer (red). Cholesterol depletion and excess are shown for each compartment. LAMP-GFP–positive endolysosomes are visibly enlarged under cholesterol excess (cf. E and F) and FR–lac-Cer–carrying vesicles appear more diffuse (C, F, and I). Bars, 4 $\mu$m.

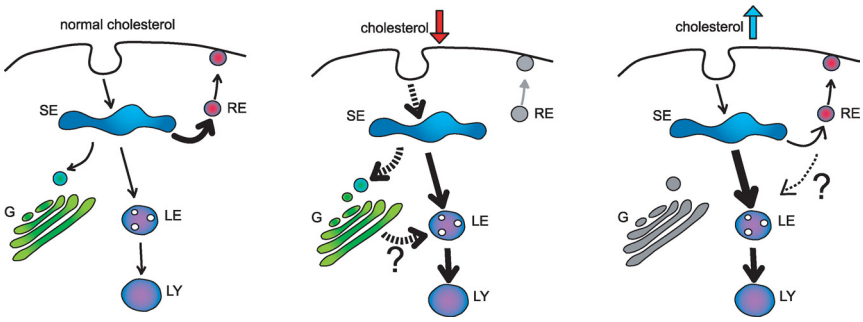


**Figure 7.** Model for cholesterol regulation of Golgi, endo-lysosomal, and recycling endosomal traffic of a glycolipid. Under normal conditions (left), the bulk of the BODIPY–lac-Cer transits from sorting endosomes (SE) to recycling endosomes (RE), whereas a smaller portion goes to Golgi (G) and late endosomes/lysosomes (LE and LY). When the cells are depleted of sterols (middle), uptake into sorting endosomes and Golgi is slower (heavy broken arrow), whereas recycling endosomes are completely bypassed. After a delay, higher than normal amounts of BODIPY–lac-Cer are found transiently in Golgi, and then endolysosomes. Question mark indicates that BODIPY–lac-Cer may be transported out of the Golgi to endolysosomes. Under cholesterol overload (right), the Golgi compartment is completely bypassed, whereas endo/lysosomes receive much more than normal BODIPY–lac-Cer and recycling endosomes somewhat less. Question mark indicates that BODIPY–lac-Cer may be transported from recycling to endolysosomes. In summary, abnormally low amounts of sterol in *Drosophila* neurons seem to favor a Golgi and lysosomal pathway at the expense of recycling, whereas excess sterol favors a lysosomal pathway mainly at the expense of Golgi.

ously reported in mammals. This could be due to species differences or to the fact that Golgi compartments and recycling endosomes lie in close proximity in some mammalian cell types (Puri *et al.*, 2001; Sabharanjak *et al.*, 2002) making localization potentially ambiguous. Because the Golgi compartment in *Drosophila* has a different, more scattered morphology than that in mammalian cells (Bard *et al.*, 2006), this may be less of a problem in the fly cells.

The most effective and long-lasting interference with uptake of BODIPY–lac-Cer in fly neurons was obtained with inhibitors of raft-mediated endocytosis and dynamin, but the clathrin inhibitor chlorpromazine also inhibited uptake nearly as strongly. The effects exerted by the rho GTPase inhibitor were only transient, by contrast. Similarly, lac-Cer in mammalian cells was shown by Pagano's group to be taken up by a dynamin- and cholesterol-dependent (presumably raft-mediated) pathway (Puri *et al.*, 2001) independent of clathrin.

The partial inhibition by the clathrin inhibitor was unexpected, given the results in mammalian cells. As a possible explanation for this, it should be noted that chlorpromazine inhibited the uptake of another presumptive raft marker CtxB to a significant extent (Broeck *et al.*, 2007), and multiple uptake mechanisms are known to operate for several other agents that are taken up by lipid rafts (Massol *et al.*, 2004; Deinhardt *et al.*, 2006).

The uptake of a glycolipid by an apparently cholesterol-mediated mechanism similar to that in mammalian cells is an important finding, given that flies are cholesterol auxotrophs and have comparatively low membrane sterol content (Marheineke *et al.*, 1998). This has led to some uncertainty as to the role of cholesterol in fly cell biology, especially with regard to its possible function in endo-lysosomal trafficking and lipid homeostasis versus a more predominant role in ecdysone hormone production (Huang *et al.*, 2005; Fluegel *et al.*, 2006; Baker and Thummel, 2007; Huang *et al.*, 2007). Although the precise roles of sterols in the fly are still unclear, lipid rafts in the form of detergent-resistant membranes rich in sphingolipids and sterols can be biochemically isolated from fly tissues, and the association of raft-localized markers can be disrupted by cholesterol extraction, as with mammalian membranes (Rietveld *et al.*, 1999; Zhai *et al.*, 2004; Hebbar *et al.*, 2008).

Another interesting outcome of this study was the identification of a phenomenon we call hijacking, which refers to the observation that BODIPY–lac-Cer can influence the trafficking of a second cargo, directing both to a novel intracellular location. This is distinct from the report of Pagano and coworkers that caveolar uptake was stimulated by by lac-Cer (Sharma *et al.*, 2004), because it involves redirection of trafficking, in this case of dextran away from the endolysosomal pathway. A similar behavior was seen between the trafficking of BODIPY–lac-Cer and another sphingolipid-interacting cargo, SBD (sphingolipid-binding domain) peptide, which when present together at the membrane trafficked nearly identically, but when incubated separately took very different routes (Steinert *et al.*, 2008). An evaluation of the universality of hijacking by glycolipids, and its utility for cellular metabolism, must await further experiments.

### *BODIPY–lac-Cer Trafficking in Drosophila Undergoes Pathway Switching in Response to Cholesterol Perturbations*

Importantly, this work has shown for the first time that in a fly neuronal culture system, the effects of cholesterol overloading on the trafficking and uptake of a simple glycolipid analogue, BODIPY–lac-Cer, is fundamentally similar to that in cholesterol-laden NPC fibroblasts, where lac-Cer trafficking is shifted in favor of the endolysosomal pathway. In contrast to human fibroblasts (Puri *et al.*, 1999), however, fly neurons can still internalize BODIPY–lac-Cer after sterol depletion, making it possible to examine changes in trafficking that are associated with loss of cholesterol as well as cholesterol overload. An unexpected result of these experiments was that both cholesterol excess and sterol depletion resulted in aberrant trafficking of BODIPY–lac-Cer, with a strong accumulation in lysosomes under both conditions after several hours. The reasons for this are as yet unclear; however, it is not known whether otherwise normal human fibroblasts might react similarly to cholesterol depletion, because in the studies of Pagano and coworkers studies, fluorescent lac-Cer's trafficking route could not be assayed because of a lack of uptake under these conditions.

In spite of the superficial similarity between the lysosomal accumulation of BODIPY–lac-Cer under cholesterol overload and depletion, it must be said that the trafficking route is clearly different when cholesterol levels are lowered, versus when they are raised (see Figure 7). Cholesterol excess allowed much more traffic through recycling compartments, but completely eliminated it from the Golgi. This is in contrast to sterol depletion, which causes complete bypass of recycling compartments, directly to sorting, Golgi, and lysosomal vesicles (summarized in Figure 7).

The results of the cholesterol overload and depletion experiments fit with a model where the uptake of glycolipid and subsequent choice between endolysosomal and recycling pathway is modulated by the level of sterol in these membranes and/or at the plasma membrane. Normally, most of the BODIPY–lac-Cer applied to the cells traffics quickly after sorting to recycling endosomes (see Figures 1 and 3), with the remainder being roughly split between late endolysosomes and Golgi. Cholesterol excess results in more BODIPY–lac-Cer being diverted gradually from a recycling pathway to accumulate in lysosomal compartments, leaving very little in the Golgi. This may be similar to the mammalian cholesterol storage situation, e.g., in NPC fibroblasts (Marks and Pagano, 2002). Under sterol depletion, the pathway is different: BODIPY–lac-Cer completely bypasses the recycling compartment and is shunted through sorting vesicles and then transiently through Golgi and finally accumulates in lysosomes. Changes in the targeting of BODIPY–lac-Cer under cholesterol perturbations may reflect a response of the cells to perceived nutritional state, causing a rerouting of internalized glycolipids that may accordingly alter lipid metabolism. As yet, a direct comparison between insect and mammalian cells' response to cholesterol loss cannot be made; thus, we do not know whether the observations in the fly model under these conditions are applicable to mammalian cells. However, the similarities in the response of glycolipid trafficking to cholesterol excess, as is seen in the case of lipid storage diseases, strongly support *Drosophila* as a valid genetic system in which to model these diseases.

## ACKNOWLEDGMENTS

We thank Lucy Cherbas and the *Drosophila* Genome Resource Center for the *Drosophila* neuronal cell line and helpful advice and Majad Khan for teaching S.H. how to do TLC. We thank Helmut Krämer (University of Texas Southwestern Medical School), Henry Chang, and Fred Bard (Institute of Molecular and Cell Biology, Agency for Science, Technology and Research, Singapore) for GFP constructs; Doris Kretzschmar (Oregon Health & Science University) and Sean Sweeney (University of York) for fly stocks; and Richard Pagano and Fred Maxfield for advice on the use of ceramide analogs and MβCD. This work was supported by the Institute of Bioengineering and Nanotechnology (Biomedical Research Council, Agency for Science, Technology and Research, Singapore) and a start-up grant from Nanyang Technological University to R.K. We thank Gayathri Sivakumar for carrying out the neuroblastoma experiment shown in Figure S4.

## REFERENCES

Baker, K. D., and Thummel, C. S. (2007). Diabetic larvae and obese flies-emerging studies of metabolism in *Drosophila*. Cell Metab. *6*, 257–266.

Bard, F., *et al.* (2006). Functional genomics reveals genes involved in protein secretion and Golgi organization. Nature *439*, 604–607.

Broeck, D. V., Lagrou, A. R., and De Wolf, M. J. (2007). Distinct role of clathrin-mediated endocytosis in the functional uptake of cholera toxin. Acta Biochim. Pol. *54*, 757–767.

Choudhury, A., Dominguez, M., Puri, V., Sharma, D. K., Narita, K., Wheatley, C. L., Marks, D. L., and Pagano, R. E. (2002). Rab proteins mediate Golgi transport of caveola-internalized glycosphingolipids and correct lipid trafficking in Niemann-Pick C cells. J. Clin. Invest. *109*, 1541–1550.

Choudhury, A., Sharma, D. K., Marks, D. L., and Pagano, R. E. (2004). Elevated endosomal cholesterol levels in Niemann-Pick cells inhibit rab4 and perturb membrane recycling. Mol. Biol. Cell *15*, 4500–4511.

Costes, S. V., Daelemans, D., Cho, E. H., Dobbin, Z., Pavlakis, G., and Lockett, S. (2004). Automatic and quantitative measurement of protein-protein colocalization in live cells. Biophys. J. *86*, 3993–4003.

Cutler, R. G., Kelly, J., Storie, K., Pedersen, W. A., Tammara, A., Hatanpaa, K., Troncoso, J. C., and Mattson, M. P. (2004). Involvement of oxidative stress-induced abnormalities in ceramide and cholesterol metabolism in brain aging and Alzheimer's disease. Proc. Natl. Acad. Sci. USA *101*, 2070–2075.

Deinhardt, K., Berninghausen, O., Willison, H. J., Hopkins, C. R., and Schiavo, G. (2006). Tetanus toxin is internalized by a sequential clathrin-dependent mechanism initiated within lipid microdomains and independent of epsin1. J. Cell Biol. *174*, 459–471.

Finley, K. D., Edeen, P. T., Cumming, R. C., Mardahl-Dumesnil, M. D., Taylor, B. J., Rodriguez, M. H., Hwang, C. E., Benedetti, M., and McKeown, M. (2003). blue cheese mutations define a novel, conserved gene involved in progressive neural degeneration. J. Neurosci. *23*, 1254–1264.

Fluegel, M. L., Parker, T. J., and Pallanck, L. J. (2006). Mutations of a *Drosophila* NPC1 gene confer sterol and ecdysone metabolic defects. Genetics *172*, 185–196.

Hebbar, S., Lee, E., Manna, M., Steinert, S., Kumar, G. S., Wenk, M., Wohland, T., and Kraut, R. (2008). A fluorescent sphingolipid binding domain peptide probe interacts with sphingolipids and cholesterol-dependent raft domains. J. Lipid Res. *49*, 1077–1089.

Holthuis, J.C.M., Pomorski, T., Raggers, R. J., Sprong, H., and Van Meer, G. (2001). The organizing potential of sphingolipids in intracellular membrane transport. Physiol. Rev. *81*, 1689–1723.

Huang, X., Suyama, K., Buchanan, J., Zhu, A. J., and Scott, M. P. (2005). A *Drosophila* model of the Niemann-Pick type C lysosome storage disease: dnpc1a is required for molting and sterol homeostasis. Development *132*, 5115–5124.

Huang, X., Warren, J. T., Buchanan, J., Gilbert, L. I., and Scott, M. P. (2007). *Drosophila* Niemann-Pick type C-2 genes control sterol homeostasis and steroid biosynthesis: a model of human neurodegenerative disease. Development *134*, 3733–3742.

Hunziker, W., and Geuze, H. J. (1996). Intracellular trafficking of lysosomal membrane proteins. Bioessays *18*, 379–389.

Klein, U., Gimpl, G., and Fahrenholz, F. (1995). Alteration of the myometrial plasma membrane cholesterol content with beta-cyclodextrin modulates the binding affinity of the oxytocin receptor. Biochemistry *34*, 13784–13793.

Koval, M., and Pagano, R. E. (1989). Lipid recycling between the plasma membrane and intracellular compartments: transport and metabolism of fluorescent sphingomyelin analogues in cultured fibroblasts. J. Cell Biol. *108*, 2169–2181.

Lim, A., and Kraut, R. (2009). The *Drosophila* BEACH family protein, blue cheese, links lysosomal axon transport with motor neuron degeneration. J. Neurosci. *29*, 951–963.

Macia, E., Ehrlich, M., Massol, R., Boucrot, E., Brunner, C., and Kirchhausen, T. (2006). Dynasore, a cell-permeable inhibitor of dynamin. Dev. Cell *10*, 839–850.

Manders, E.M.M., Verbeek, F. J., and Aten, J. A. (1993). Measurement of co-localization of objects in dual-color confocal images. J. Microsc. *169*, 375–382.

Marheineke, K., Grünewalda, S., Christie, W., and Reiländer, H. (1998). Lipid composition of *Spodoptera frugiperda* (Sf9) and *Trichoplusia ni* (Tn) insect cells used for baculovirus infection. FEBS Lett. *441*, 49–52.

Marks, D. L., and Pagano, R. E. (2002). Endocytosis and sorting of glycosphingolipids in sphingolipid storage disease. Trends Cell Biol. *12*, 605–613.

Martin, O. C., and Pagano, R. E. (1994). Internalization and sorting of a fluorescent analogue of glucosylceramide to the Golgi apparatus of human skin fibroblasts: utilization of endocytic and nonendocytic transport mechanisms. J. Cell Biol. *125*, 769–781.

Massol, R. H., Larsen, J. E., Fujinaga, Y., Lencer, W. I., and Kirchhausen, T. (2004). Cholera toxin toxicity does not require functional Arf6- and dynamin-dependent endocytic pathways. Mol. Biol. Cell *15*, 3631–3641.

Maxfield, F. R., and Tabas, I. (2005). Role of cholesterol and lipid organization in disease. Nature *438*, 612–621.

Min, K. T., and Benzer, S. (1997). Spongecake and eggroll: two hereditary diseases in *Drosophila* resemble patterns of human brain degeneration. Curr. Biol. *7*, 885–888.

Mukherjee, S., and Maxfield, F. R. (2004). Lipid and cholesterol trafficking in NPC. Biochim. Biophys. Acta *1685*, 28–37.

Myllykangas, L., Tyynela, J., Page-McCaw, A., Rubin, G. M., Haltia, M. J., and Feany, M. B. (2005). Cathepsin D-deficient *Drosophila* recapitulate the key features of neuronal ceroid lipofuscinoses. Neurobiol. Dis. *19*, 194–199.

Nakano, Y., *et al.* (2001). Mutations in the novel membrane protein spinster interfere with programmed cell death and cause neural degeneration in *Drosophila melanogaster*. Mol. Cell. Biol. *21*, 3775–3788.

Pagano, R. E. (2003). Endocytic trafficking of glycosphingolipids in sphingolipid storage diseases. Philos. Trans. R. Soc. Lond. B. Biol. Sci. *358*, 885–891.

Phillips, S. E., Woodruff, E. A., 3rd, Liang, P., Patten, M., and Broadie, K. (2008). Neuronal loss of *Drosophila* NPC1a causes cholesterol aggregation and age-progressive neurodegeneration. J. Neurosci. *28*, 6569–6582.

Puglielli, L., Tanzi, R. E., and Kovacs, D. M. (2003). Alzheimer's disease: the cholesterol connection. Nat. Neurosci. *6*, 345–351.

Pulipparacharuvil, S., Akbar, M. A., Ray, S., Sevrioukov, E. A., Haberman, A. S., Rohrer, J., and Kramer, H. (2005). *Drosophila* Vps16A is required for trafficking to lysosomes and biogenesis of pigment granules. J. Cell Sci. *118*, 3663–3673.

Puri, V., Jefferson, J. R., Singh, R. D., Wheatley, C. L., Marks, D. L., and Pagano, R. E. (2003). Sphingolipid storage induces accumulation of intracellular cholesterol by stimulating SREBP-1 cleavage. J. Biol. Chem. *278*, 20961–20970.

Puri, V., Watanabe, R., Dominguez, M., Sun, X., Wheatley, C. L., Marks, D. L., and Pagano, R. E. (1999). Cholesterol modulates membrane traffic along the endocytic pathway in sphingolipid-storage diseases. Nat. Cell Biol *1*, 386–388.

Puri, V., Watanabe, R., Singh, R. D., Dominguez, M., Brown, J. C., Wheatley, C. L., Marks, D. L., and Pagano, R. E. (2001). Clathrin-dependent and -independent internalization of plasma membrane sphingolipids initiates two Golgi targeting pathways. J. Cell Biol. *154*, 535–547.

Rietveld, A., Neutz, S., Simons, K., and Eaton, S. (1999). Association of sterol- and glycosylphosphatidylinositol-linked proteins with *Drosophila* raft lipid microdomains. J. Biol. Chem. *274*, 12049–12054.

Sabharanjak, S., Sharma, P., Parton, R. G., and Mayor, S. (2002). GPI-anchored proteins are delivered to recycling endosomes via a distinct cdc42-regulated, clathrin-independent pinocytic pathway. Dev. Cell *2*, 411–423.

Seppo, A., Moreland, M., Schweingruber, H., and Tiemeyer, M. (2000). Zwitterionic and acidic glycosphingolipids of the *Drosophila melanogaster* embryo. Eur. J. Biochem. *267*, 3549–3558.

Sharma, D. K., Brown, J. C., Choudhury, A., Peterson, T. E., Holicky, E., Marks, D. L., Simari, R., Parton, R. G., and Pagano, R. E. (2004). Selective stimulation of caveolar endocytosis by glycosphingolipids and cholesterol. Mol. Biol. Cell *15*, 3114–3122.

Sharma, D. K., Choudhury, A., Singh, R. D., Wheatley, C. L., Marks, D. L., and Pagano, R. E. (2003). Glycosphingolipids internalized via caveolar-related endocytosis rapidly merge with the clathrin pathway in early endosomes and form microdomains for recycling. J. Biol. Chem. *278*, 7564–7572.

Sillence, D. J., Puri, V., Marks, D. L., Butters, T. D., Dwek, R. A., Pagano, R. E., and Platt, F. M. (2002). Glucosylceramide modulates membrane traffic along the endocytic pathway. J. Lipid Res. *43*, 1837–1845.

Simonsen, A., Cumming, R. C., Lindmo, K., Galaviz, V., Cheng, S., Rusten, T. E., and Finley, K. D. (2007). Genetic modifiers of the *Drosophila* blue cheese gene link defects in lysosomal transport with decreased life span and altered ubiquitinated-protein profiles. Genetics *176*, 1283–1297.

Singh, R. D., Puri, V., Valiyaveettil, J. T., Marks, D. L., Bittman, R., and Pagano, R. E. (2003). Selective caveolin-1-dependent endocytosis of glycosphingolipids. Mol. Biol. Cell *14*, 3254–3265.

Sriram, V., Krishnan, K. S., and Mayor, S. (2003). deep-orange and carnation define distinct stages in late endosomal biogenesis in *Drosophila melanogaster.* J. Cell Biol. *161*, 593–607.

Steinert, S., *et al.* (2008). A fluorescent glycolipid-binding peptide probe traces cholesterol dependent microdomain-derived trafficking pathways. PLoS ONE *3*, e2933.

te Vruchte, D., Lloyd-Evans, E., Veldman, R. J., Neville, D. C., Dwek, R. A., Platt, F. M., van Blitterswijk, W. J., and Sillence, D. J. (2004). Accumulation of glycosphingolipids in Niemann-Pick C disease disrupts endosomal transport. J. Biol. Chem. *279*, 26167–26175.

Tschape, J. A., Hammerschmied, C., Muhlig-Versen, M., Athenstaedt, K., Daum, G., and Kretzschmar, D. (2002). The neurodegeneration mutant lochrig interferes with cholesterol homeostasis and Appl processing. EMBO J. *21*, 6367–6376.

Ui, K., Nishihara, S., Sakuma, M., Togashi, S., Ueda, R., Miyata, Y., and Miyake, T. (1994). Newly established cell lines from *Drosophila* larval CNS express neural specific characteristics. In Vitro Cell Dev. Biol. Anim. *30A*, 209–216.

Wiegandt, H. (1992). Insect glycolipids. Biochim. Biophys. Acta Lipids Lipid Metab. *1123*, 117–126.

Wolozin, B. (2004). Cholesterol and the biology of Alzheimer's disease. Neuron *41*, 7–10.

Zhai, L., Chaturvedi, D., and Cumberledge, S. (2004). *Drosophila* wnt-1 undergoes a hydrophobic modification and is targeted to lipid rafts, a process that requires porcupine. J. Biol. Chem. *279*, 33220–33227.